7332–7342 Nucleic Acids Research, 2010, Vol. 38, No. 20 Published online 8 July 2010
doi:10.1093/nar/gkq600

Double-stranded DNA-templated cleavage of oligonucleotides containing a P3′→N5′ linkage triggered by triplex formation: the effects of chemical modifications and remarkable enhancement in reactivity

Kosuke Ramon Ito[1], Tetsuya Kodama[1], Masaharu Tomizu[1], Yoshinori Negoro[1], Ayako Orita[1], Tomohisa Osaki[1], Noritsugu Hosoki[1], Takaya Tanaka[1], Takeshi Imanishi[1] and Satoshi Obika[1,2,*]

[1]Graduate School of Pharmaceutical Sciences, Osaka University, 1-6 Yamadaoka, Suita, Osaka 565-0871 and [2]PRESTO, JST, Sanbancho Building 5-sanbancho, Chiyodaku, Tokyo 102-0075, Japan

Received February 5, 2010; Revised June 9, 2010; Accepted June 20, 2010

ABSTRACT

We recently reported double-stranded DNA-templated cleavage of oligonucleotides as a sequence-specific DNA-detecting method. In this method, triplex-forming oligonucleotides (TFOs) modified with 5′-amino-2′,4′-BNA were used as a DNA-detecting probe. This modification introduced a P3′→N5′ linkage (P–N linkage) in the backbone of the TFO, which was quickly cleaved under acidic conditions when it formed a triplex. The prompt fission of the P–N linkage was assumed to be driven by a conformational strain placed on the linkage upon triplex formation. Therefore, chemical modifications around the P–N linkage should change the reactivity by altering the microenvironment. We synthesized 5′-aminomethyl type nucleic acids, and incorporated them into TFOs instead of 5′-amino-2′,4′-BNA to investigate the effect of 5′-elongation. In addition, 2′,4′-BNA/LNA or 2′,5′-linked DNA were introduced at the 3′- and/or 5′-neighboring residues of 5′-amino-2′,4′-BNA to reveal neighboring residual effects. We evaluated the triplex stability and reaction properties of these TFOs, and found out that chemical modifications around the P–N linkage greatly affected their reaction properties. Notably, 2′,5′-linked DNA at the 3′ position flanking 5′-amino-2′,4′-BNA brought significantly higher reactivity, and we succeeded in indicating that a TFO with this modification is promising as a DNA analysis tool.

INTRODUCTION

DNA-templated reactions have been widely used not only in the area of DNA sensing (1–23) but also for synthesis and selection of small molecules (24–27). The reaction on the template would reflect the microenvironment around the reactive site. In fact, especially in the area of DNA sensing *via* DNA-templated reactions, probes with delicate modifications, which will change the microenvironment around the reactive site, have exhibited dramatic differences in their reactivity, sequence selectivity, and/or turnover numbers (1–6). These observations suggest that it is important to optimize the reactivity of the probes to make these analytical tools practical.

We recently reported on a double-stranded DNA (dsDNA)-templated cleavage of oligonucleotides as a sequence-specific DNA detecting method (28). In this method, triplex-forming oligonucleotides (TFOs) modified with 5′-amino-2′-*O*,4′-*C*-methylene bridged nucleic acid (5′-amino-2′,4′-BNA) were used (28). This modification introduced a P–N linkage in the backbone of the TFO, instead of the P–O linkage generally found in phosphodiester moieties of oligonucleotides. Although it is well known that a P–N linkage is cleavable under mild acidic conditions (29), we found out that the cleaving reaction of the P–N linkage was greatly accelerated

*To whom correspondence should be addressed. Tel: +81 6 6879 8200; Fax: +81 6 6879 8204; Email: obika@phs.osaka-u.ac.jp

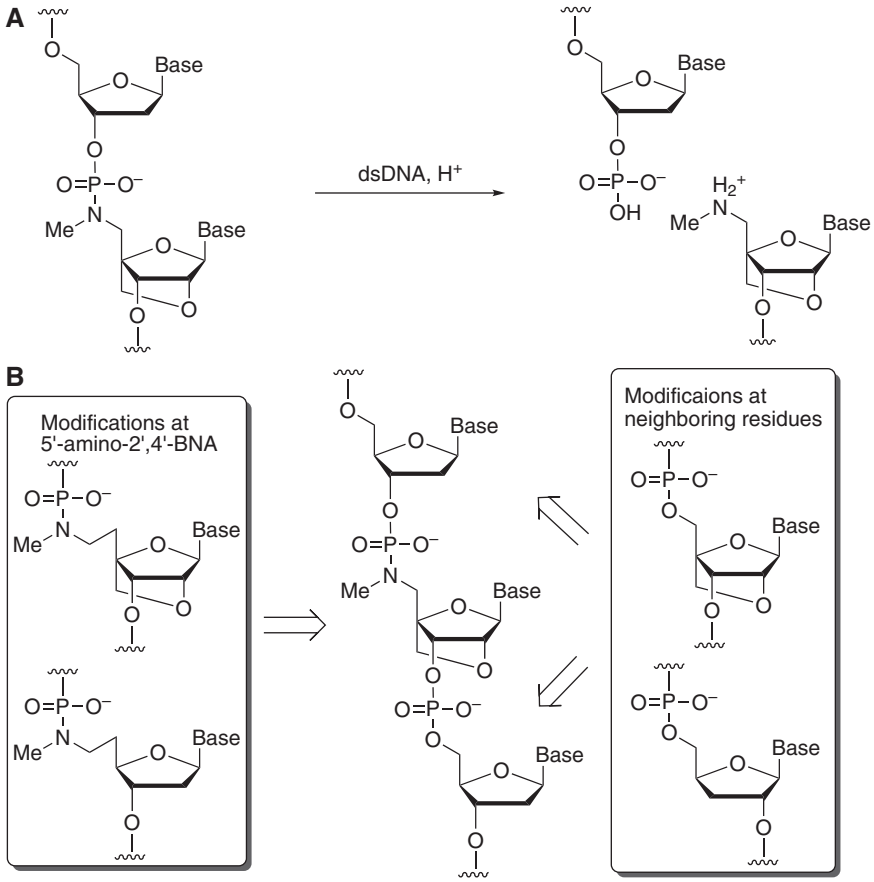

Scheme 1. (**A**) Target dsDNA and acids act as catalysts for the cleavage of the P–N linkage. (**B**) Strategy to change the microenvironment around the P-N linkage.

when the TFO formed a triplex with its target dsDNA in a sequence-specific manner under mild acidic conditions (Scheme 1A) (28,30). We demonstrated that this dsDNA-templated cleavage combined with fluorescence resonance energy transfer (FRET) technology was useful as a DNA detecting method, distinguishing a single nucleotide mismatch (28).

Because the rate of the reaction is an important factor for sensitivity and quickness of the analysis, we became interested in enhancing the reactivity of the probe. In a previous report, we proposed that the acid-mediated cleavage of the P–N linkage triggered by triplex formation should be driven by a conformational strain on the P–N linkage (28). This interested us in the effects of modifications in changing the microenvironment around the P–N linkage. In the present study, we investigated the relationship between those chemical modifications and the reactivity of the acid-mediated cleavage of TFOs triggered by triplex formation. At first, we synthesized 5′-aminomethyl-type nucleic acids, and incorporated them into TFOs instead of 5′-amino-2′,4′-BNA to investigate the effect of 5′-elongation (Scheme 1B, left). We also synthesized oligonucleotides containing 2′-*O*,4′-*C*-methylene bridged nucleic acid (2′,4′-BNA)/locked nucleic acid (LNA) (31–34) or 2′,5′-linked DNA (35,36) as 5′ and/or 3′ neighboring residues of 5′-amino-2′,4′-BNA in TFO to reveal the neighboring residual effects (Scheme 1B, right). Here we revealed the effects of chemical modifications around the P–N linkage on dsDNA-templated cleavage of TFO, and detailed investigation was performed on one of the eminent TFOs to elucidate its potential as an analytical tool.

MATERIALS AND METHODS

General aspects and instrumentations

Natural oligonucleotides, such as the target dsDNAs 5′-d(GCTAAAAAGAMAGAGAGATCG)-3′, 5′-d(CGA TCTCTCTNTCTTTTTAGC)-3′, where M and N were A, C, G or T; and **TFO0** 5′-d(TTTTTCTTTCTCTCT)-3′, where C represents 2′-deoxy-5-methylcytidine, were purchased from Hokkaido System Science Co., Ltd and Gene Design Inc, respectively. The stoichiometry of oligonucleotides was calculated using the following extinction coefficients (l/mol/cm); A, 15000; G, 12500; C, 7500; T, 8500; 5-MeC, 6000.

Syntheses of TFOs

TFO′ and **TFO*** were prepared according to previous reports (28,29). Syntheses of **TFO1–TFO9** were performed at a 0.2 μmol scale on an automated DNA synthesizer

(Applied Biosystems, Expedite™ 8909) using the standard phosphoramidite protocol on CPG supports except for coupling time of certain couplings (90 s in the standard protocol). The coupling time of amidite **9**, **15** and 5′-amino-2′,4′-BNA-T (NMe) amidite was extended to 15, 15 and 10 min, respectively. In addition, the coupling time for P–N bond formation in **TFO3**, **TFO5**, **TFO6** and **TFO8** was extended to 5 min. The phosphoramidite derivatives of 2′,4′-BNA-T (34), which is also commercially available as LNA, and 5′-amino-2′,4′-BNA-T (NMe) (28) were prepared according to previous reports. The phosphoramidite derivative monomer of 2′,5′-linked DNA-T (3′-dT CE phosphoramidite) was purchased from Glen Research. Other reagents for oligonucleotide synthesis were purchased from Proligo. As an activator, 1*H*-tetrazole was used for every coupling step. Syntheses of TFOs were performed on DMTr-OFF mode. Cleavage from the CPG support was accomplished using 28% aqueous ammonia solution at room temperature for 1.5 h, and the solution containing TFO was kept at 55°C for 20 h. The crude TFOs were purified with a gel filtration column (General Electric Company, NAP™ 10 Column) and RP-HPLC (Waters Xterra™ MS C_{18}, 2.5 μm 10 × 50 mm) [buffer **A**, 0.1 M TEAA (pH 7.0); Buffer **B**, 0.1 M TEAA (pH 7.0) /MeCN = 1:1; linear gradient, **B** 12–24%/30 min; flow rate, 3.0 ml/min]. The composition of TFOs was confirmed by MALDI–TOF–MS analysis using 3-hydroxypicolinic acid and diammonium hydrogen citrate as the matrix. The isolated yield and MALDI–TOF–MS data for **TFO1–TFO9** were summarized in Supplementary Table S1.

UV melting experiments

UV melting experiments were carried out on SHIMADZU UV-1650PC, and SHIMADZU UV-1650B spectrometers. The UV melting profiles were recorded in a solution whose pH was 6.0 or 4.0. The pH 6.0 solution contained 140 mM KCl, 10 mM $MgCl_2$, 1.0 mM sodium phosphate buffer, 10 mM sodium citrate buffer, and was used for **TFO′**, **TFO*** and **TFO0–TFO9**. The pH 4.0 solution contained 140 mM KCl, 10 mM $MgCl_2$, 1.0 mM sodium phosphate buffer, 10 mM sodium citrate–HCl buffer and was used for **TFO0**. The final pH was actually measured using Twin pH Meter B-212 (Horiba, Ltd). The scan rate was 0.5°C/min with detection at 260 nm. The final concentration of each oligonucleotide was 1.5 μM, which was calculated from the extinction coefficients. The solution containing oligonucleotides was heated and subsequently cooled to 10°C to generate the triplex. The melting temperatures were obtained as maxima of the first derivative of the melting curve.

General methods for hydrolysis experiments

An amount of 2.0 μl of 50 mM sodium phosphate buffer (pH 7.0), 10 μl of 100 mM $MgCl_2$, 14 μl of 1.0 M KCl, 13.4 μl of 25 μM TFO with or without 13.4 μl of 25 μM target dsDNA were mixed, and deionized water was added to adjust the volume to 90 μl. This solution was maintained at 40°C, after being heated and subsequently cooled to generate a triplex. Then, 10 μl of 100 mM sodium citrate-based buffer was added for acidification, and the final composition of the solution was 140 mM KCl, 1.0 mM sodium phosphate buffer, 10 mM sodium citrate-based buffer, 10 mM $MgCl_2$ and 3.35 μM each strand. The final pH was actually measured using Twin pH Meter B-212 (Horiba, Ltd). After the incubation for the indicated amount of time at 40°C, 10 μl of the reaction mixture was removed, added to 160 μl of 0.10 M triethylammonium acetate buffer (pH 9.0) to stop the reaction, and analyzed by HPLC system (Shimadzu Prominence) to determine the proportion of intact TFO. Replacement of KCl with NaCl or exclusion of $MgCl_2$ from reaction mixture did not have significant effects on the reactivity (data not shown). The HPLC system used for the analysis of the reaction is described in the Supplementary Data.

Kinetics of acid-mediated cleavage of TFOs triggered by triplex formation

The reaction was performed as is described in the general method for hydrolysis experiments. An amount of 10 μl of 100 mM sodium citrate–HCl buffer (pH 4.0) was used to adjust the pH to 4.0. The reaction mixture was incubated for 0, 5, 10, 20 and 60 min (**TFO1–TFO9**), or 0, 30, 60, 120 and 240 min (**TFO′**).

Effects of pH on reactivity

The reaction was performed as described in the general method for hydrolysis experiments. The reactivity at different pH was evaluated for **TFO4** and **TFO8** with the full match target dsDNA. 10 μl of 100 mM sodium citrate–HCl buffers (pH 4.5 and 5.0) were used to adjust the pH to 4.3 and 4.5, and 10 μl of 100 mM sodium citrate buffer (pH 5.5) was used to adjust the pH to 4.9. The reaction mixture was incubated for 0, 5, 10, 20 and 60 min.

Sequence selectivity

The reaction was performed as described in the general method for hydrolysis experiments. The sequence selectivity of **TFO8** was evaluated in the presence of full match, misT, misC and misG target dsDNAs (Figure 1) or in the absence of the target dsDNA, and 10 μl of 100 mM sodium citrate–HCl buffer (pH 3.0) was used to adjust the pH to 3.3. The reaction mixture was incubated for 2 min.

Molecular modeling

As the initial structure, the triplex containing dsDNA (5′-AAAAAGAAAGAGAGA-3′/3′-TTTTTCTTTCTCT CT-5′) and **TFO0** was generated with default parameters of Discovery Studio 2.5™ (Accelrys Software, Inc.).

TFO binding site

5'-d(GCTAAAAAGAMAGAGAGATCG)-3'
3'-d(CGATTTTTCTNTCTCTCTAGC)-5'

Figure 1. Sequence of the target dsDNA used in the present study. Bar indicates a site where each TFO could bind. MN: AT (full match), TA (misT), CG (misC), GC (misG).

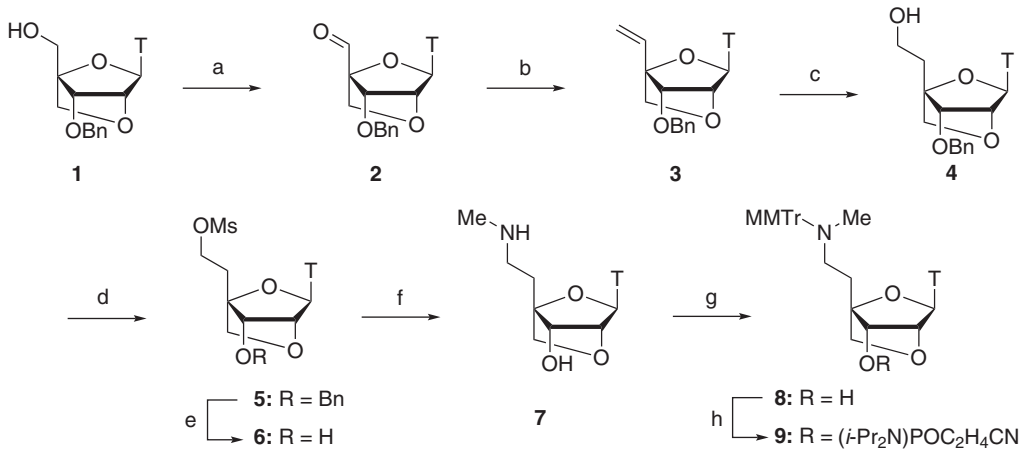

Scheme 2. Reagents and conditions: (a) Dess-Martin reagent, CH_2Cl_2, rt, 1 h; (b) Ph_3PBrCH_3, *n*-BuLi, THF, rt, 1 h, 57% over two steps; (c) BH_3, THF, NaOH, H_2O_2, rt, 40 min, 50%; (d) MsCl, pyridine, rt, 1 h, 87%; (e) $Pd(OH)_2$-C, cyclohexene, EtOH, reflux, 3 h; (f) liquid $MeNH_2$ in a sealed tube, rt, 62 h; (g) MMTrCl, Et_3N, pyridine, rt, 2 h, 83% over three steps; (h) $(i\text{-}Pr_2N)_2POCH_2CH_2CN$, diisopropylammonium tetrazolide, MeCN/THF, rt, 10 h, 85%. T, thymin-1-yl.

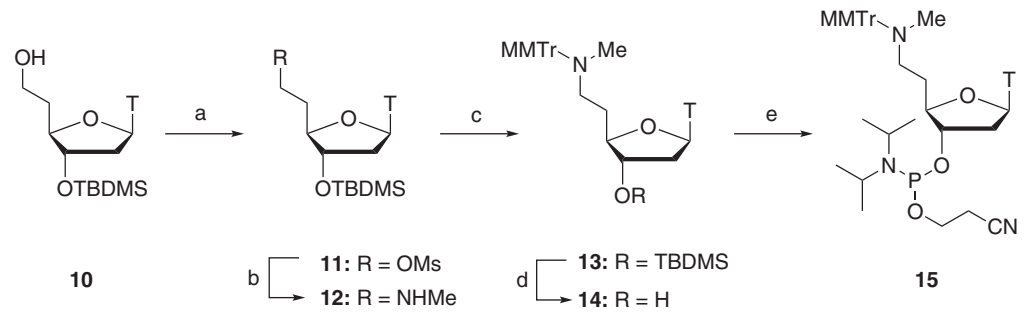

Scheme 3. Reagents and conditions: (a) MsCl, pyridine, rt, 1 h, 85%; (b) liquid $MeNH_2$ in a sealed tube, rt, 48 h; (c) MMTrCl, Et_3N, pyridine, rt, 2 h, 93% over two steps; (d) TBAF, THF, rt, 1.5 h, 72%; (e) $(i\text{-}Pr_2)N_2POCH_2CH_2CN$, diisopropylammonium tetrazolide, MeCN/THF, rt, 13 h, 87%. T, thymin-1-yl.

Then, the structure of **TFO*** was constructed by the replacement of the P–O linkage in the middle of the sequence of **TFO0** with the P–N linkage, and insertion of O2′ atom and methylene bridge over O2′ and C4′ atom. The obtained triplex structure was exported to MacroModel 9.1^{TM} (Schrödinger, LLC), and it was modified to each triplex structure (**TFO7**, **TFO8** and **TFO9**). On each structure (**TFO***, **TFO7**, **TFO8** and **TFO9**) was performed energy minimization using AMBER* as a force field and GB/SA solvation model of water as implemented in MacroModel 9.1^{TM}. The minimization was performed using PRCG method to obtain structures optimized to within a gradient of 0.05 kJ/mol Å.

RESULTS

Synthesis of 5′-aminomethyl-2′,4′-BNA (NMe)

As shown in Scheme 2, the synthesis of an amidite **9** was performed starting from **1** (37). Utilizing the Dess-Martin reagent, **1** was oxidized to give an aldehyde **2**, which was treated with methyltriphenylphosphonium bromide to give a 4′-vinyl nucleoside **3**. Hydroboration followed by oxidation gave an 5′-elongated nucleoside **4**. After mesylation of the hydroxy group of **4**, the 3′-benzyl group was removed by $Pd(OH)_2$-catalized hydrogenolysis to give **6**. The mesylate group of **6** was substituted to a methylamino group by treating with methylamine in a sealed tube to give an 5′-aminomethyl nucleoside analogue **7**. The 4-methoxytritylation of **7** treated with 4-methoxytrityl chloride (MMTrCl) followed by phosphitylation gave an amidite **9**. The procedure for the synthesis is described in the Supplementary Data.

Synthesis of 5′-aminomethyl-DNA (NMe)

The synthesis of an amidite **15** was performed from **10** (38) in a similar manner to that of an amidite **9** as shown in Scheme 3. Mesylation of the hydroxy group of **10** followed by substitution to a methylamino group gave **12**. 4-Methoxytritylation, removal of the TBDMS group followed by phosphitylation afforded an amidite **15**. The procedure for the synthesis is described in the Supplementary Data.

Syntheses of TFOs

TFO1–TFO9 were synthesized by conventional phosphoramidite chemistry on an automated DNA synthesizer

Table 1. Sequences, T_m values and hydrolysis rate constants of each TFO

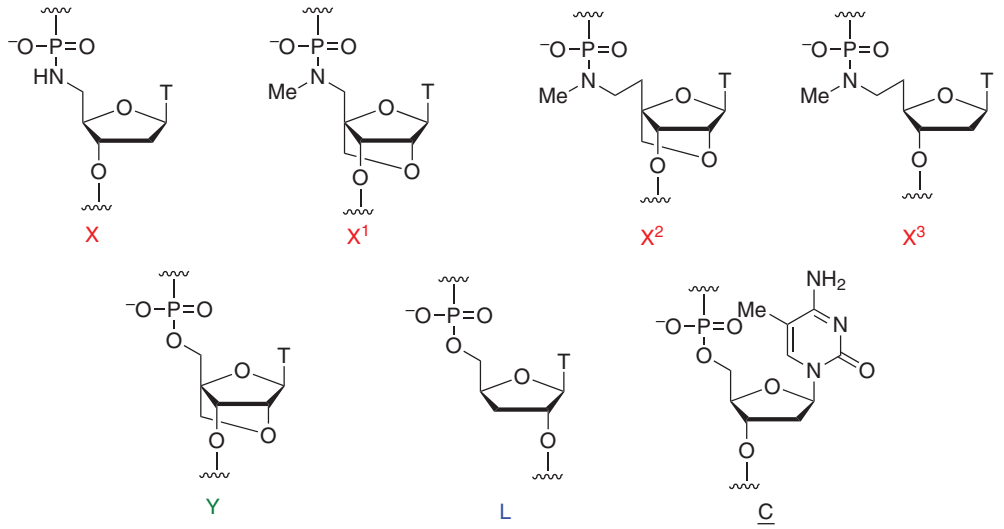

TFO	Sequence[a]	T_m (°C)	$k_{triplex} \times 10^3$ (s^{-1})	$k_{alone} \times 10^3$ (s^{-1})	$k_{triplex}/k_{alone}$
TFO′	5′-d(TTTTTCTXTCTCTCT)-3′	57	0.17 ± 0.03	0.034 ± 0.004	5.0 ± 1.1
TFO*	5′-d(TTTTTCTX[1]TCTCTCT)-3′	61	0.77 ± 0.03[b]	0.027 ± 0.005[b]	29 ± 5
TFO0	5′-d(TTTTTCTTTCTCTCT)-3′	59 (71)[c]	–	–	–
TFO1	5′-d(TTTTTCTX[2]TCTCTCT)-3′	61	0.57 ± 0.20	0.089 ± 0.020	6.4 ± 2.6
TFO2	5′-d(TTTTTCTX[3]TCTCTCT)-3′	52	2.0 ± 0.5	0.075 ± 0.005	27 ± 7
TFO3	5′-d(TTTTTCYX[1]TCTCTCT)-3′	65	0.051 ± 0.013	0.017 ± 0.006	3.1 ± 1.4
TFO4	5′-d(TTTTTCTX[1]YCTCTCT)-3′	63	1.4 ± 0.4	0.038 ± 0.012	37 ± 13
TFO5	5′-d(TTTTTCYX[1]YCTCTCT)-3′	75	0.044 ± 0.025	0.026 ± 0.003	1.7 ± 1.0
TFO6	5′-d(TTTTYCTX[1]TCYCTCT)-3′	66	1.3 ± 0.4	0.029 ± 0.004	45 ± 14
TFO7	5′-d(TTTTTCLX[1]TCTCTCT)-3′	53	n.d.[d]	0.066 ± 0.024	n.d.[d]
TFO8	5′-d(TTTTTCTX[1]LCTCTCT)-3′	61	2.1 ± 0.1	0.022 ± 0.002	96 ± 9
TFO9	5′-d(TTTTTCLX[1]LCTCTCT)-3′	52	0.022 ± 0.012	0.058 ± 0.003	0.37 ± 0.21

Conditions for T_m analysis: 140 mM KCl, 10 mM $MgCl_2$, 1.0 mM sodium phosphate buffer, 10 mM sodium citrate buffer and 1.5 μM each strand, the final pH 6.0; the T_m value of the underlying target dsDNA was 61°C. Conditions for hydrolysis experiments: 140 mM KCl, 10 mM $MgCl_2$, 1.0 mM sodium phosphate buffer, 10 mM sodium citrate–HCl buffer, and 3.35 μM each strand, 40°C, the final pH 4.0; the average of pseudo-first order rate constant is shown with standard deviation (n = 3–4).

[a]X, 5′-amino-DNA-T (NH); X^1, 5′-amino-2′,4′-BNA-T (NMe); X^2, 5′-aminomethyl-2′,4′-BNA-T (NMe); X^3, 5′-aminomethyl-DNA-T (NMe); Y, 2′,4′-BNA/LNA-T; L, 2′,5′-linked DNA-T; C, 2′-deoxy-5-methylcytidine.

[b]From a previous report (28).

[c]Figure in the parenthesis represents T_m in acidic conditions (140 mM KCl, 10 mM $MgCl_2$, 1.0 mM sodium phosphate buffer, 10 mM sodium citrate–HCl buffer and 1.5 μM each strand, the final pH 4.0).

[d]The reaction rate constant could not be determined because the cleavage was too slow.

as described in the Materials and methods section. The TFOs were purified by reversed-phase HPLC (RP-HPLC) and characterized by MALDI–TOF–MS. Cleavage of **TFO1** took place under measurement of MALDI–TOF–MS, and only fragment signals were observed instead of intact ones. Therefore, the composition of **TFO1** was confirmed by its fragments signal. The sequences of each TFO are given in Table 1.

Thermal stability of TFOs in triplexes

Initially, we investigated the triplex-forming ability of **TFO′**, **TFO*** and **TFO0–TFO9** by means of UV melting experiments, and the T_m values of triplexes containing the full match target dsDNA (Figure 1) and each TFO are summarized in Table 1. Although we wished to evaluate the triplex stability of each TFO under the conditions used in the hydrolysis experiments, it was not possible due to the cleavage of the P–N linkage. Therefore, we performed the melting experiments at less acidic pH (pH 6.0). At the same time the T_m value of **TFO0**, which contains no P–N linkage, was examined under acidic conditions (pH 4.0). Since triplex formation requires the protonation on the cytidines in TFO, the T_m of a triplex is known to increase in proportion to the decrease of pH (39,40). Hence, we supposed that it would be able to estimate the triplex-forming ability of the other TFOs containing the P–N linkage under acidic conditions, comparing the T_m values of **TFO0** at pH 4.0 and 6.0. At pH 6.0, triplexes melted directly to single-stranded state, except for **TFO2**, **TFO7**, and **TFO9** (Supplementary Figure S1). T_m of the target dsDNA was also measured, and found to be 61°C. The T_m values of **TFO′**, and **TFO*** were 57 and 61°C while

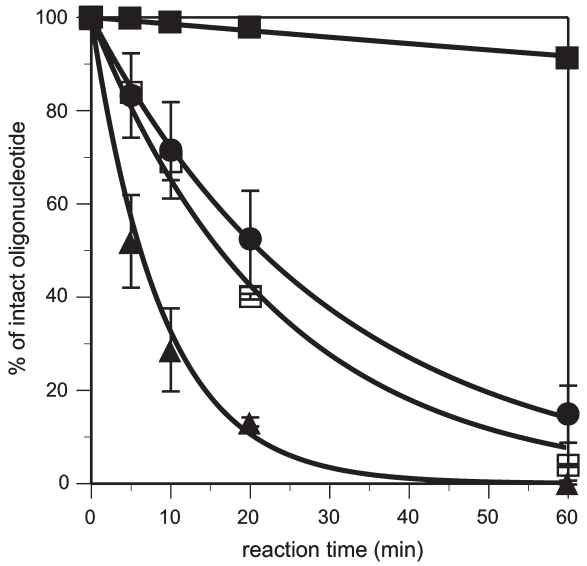

Figure 2. Time-course of the cleavage of **TFO1**, **TFO2** and **TFO***. **TFO1** (filled circles), **TFO2** (filled triangles) and **TFO*** (open squares) with the target dsDNA, respectively, and **TFO*** (filled squares) without the target dsDNA. Error bars indicate standard deviation ($n = 3$–4). The data for **TFO*** were obtained from a previous report (28). Conditions: 140 mM KCl, 10 mM $MgCl_2$, 1.0 mM sodium phosphate buffer, 10 mM sodium citrate–HCl buffer and 3.35 μM each strand, 40°C, the final pH 4.0.

those of **TFO1–TFO9** were 61, 52, 65, 63, 75, 66, 53, 61 and 52°C, respectively (Table 1). As is well known (39–41), acidic conditions greatly stabilized triplex containing **TFO0** (T_m; 59°C at pH 6.0 to 71°C at pH 4.0). While the thermal stability of the triplex containing **TFO1** was as the same with that of **TFO***, the removal of the 2′,4′-bridge led to lower triplex stability (**TFO2**). As previously reported (34), 2′,4′-BNA/LNA modifications (**TFO3–TFO6**) stabilized the triplex. TFOs modified with 2′,5′-linked DNA exhibited a less or equivalent triplex-forming ability depending on the modification positions (**TFO7**, **TFO8** and **TFO9**) compared to **TFO***. Considering the triplex-forming ability of **TFO0** under acidic conditions, we estimated that almost all the fraction of **TFO′**, **TFO*** and **TFO1–TFO9** formed triplexes at pH 4.0, 40°C.

Evaluation of reactivity of TFOs

To reveal the effects of the chemical modifications on dsDNA-templated cleavage of TFOs, the reactivity of **TFO′** and **TFO1–TFO9** was investigated at pH 4.0, 40°C. Each TFO was annealed with the target dsDNA to form a triplex, which was followed by acidification to start the reaction, and the remaining amount of intact TFO was analyzed by HPLC (Supplementary Figure S2). A time-course of the cleavage of each TFO is shown in Figure 2 and Supplementary Figure S3, and the pseudo-first order rate constants of the cleaving reaction in the presence ($k_{triplex}$) or the absence (k_{alone}) of the target dsDNA are summarized in Table 1.

As shown in Figure 2 and Table 1, **TFO1** exhibited almost the same reactivity with **TFO***, and **TFO2** exhibited higher reactivity than **TFO*** in the presence of the target dsDNA. On the other hand, in the absence of the target dsDNA, 5′-aminomethyl-modified **TFO1** and **TFO2** both exhibited higher reactivity than any other TFOs studied here.

Table 1 shows that the 2′,4′-BNA/LNA modification (Y) at the 5′-neighboring residue of 5′-amino-2′,4′-BNA (X^1) (**TFO3** and **TFO5**) significantly reduced the reactivity, while the modification at the 3′ neighboring residue (**TFO4**) enhanced the reactivity in the presence of the target dsDNA compared to that of **TFO***. The TFO containing two 2′,4′-BNA/LNA residues separately (**TFO6**) showed as high reactivity as **TFO4** in the presence of the target dsDNA.

Although the reactivity of the TFOs modified with 2′,4′-BNA/LNA varied by their modification patterns in the presence of the target dsDNA, the reactivity in the single-stranded state was not affected by these modifications.

2′,5′-Linked DNA-modified TFOs showed somewhat similar tendency to 2′,4′-BNA/LNA-modified TFOs (Table 1). In the presence of the target dsDNA, the modification with 2′,5′-linked DNA (L) at the 5′-neighboring residue (**TFO7** and **TFO9**) significantly reduced the reactivity, while the 2′,5′-linked DNA modification at the 3′ neighboring residue of 5′-amino-2′,4′-BNA (**TFO8**) brought the highest reactivity.

In the absence of the target dsDNA, the reactivity of **TFO7** and **TFO9** was higher than that of **TFO***, and their reaction rates overtook those in the presence of the target dsDNA. On the other hand, the reactivity of **TFO8** was quite low in the absence of the target dsDNA.

The relative pseudo-first order rate constants ($k_{triplex}/k_{alone}$) could be an important factor of sensitivity. Therefore, the ratios were calculated for each TFO, and these values are given in Table 1. Notably, the ratio of **TFO8** was the highest to be 96 ± 9 (that of **TFO′** and **TFO*** was 5.0 ± 1.1 and 29 ± 5, respectively), which indicated that the sensitivity of **TFO8** would be ∼20 times and three times higher than that of **TFO′** and **TFO***.

Effect of pH on the reactivity

The kinetics at different pH was evaluated to elucidate the detail reaction properties of **TFO8** (5′-TX^1L-3′) in the triplex form. We performed the reaction at pH 4.3, 4.5 and 4.9 in addition to pH 4.0. As a comparison, **TFO4** (5′-TX^1Y-3′) was also evaluated under the same conditions. This **TFO4** was chosen because it was modified as the same way with **TFO8** (modified at 3′-neighboring residue of 5′-amino-2′,4′-BNA), and the reaction rates of **TFO8** and **TFO4** were suitable to be monitored under the same reaction time range. Pseudo-first order rate constants (k_{obs}) obtained from the experiments at different pH were plotted against proton concentration ($[H^+]$) to reveal their mode of the pH dependency (Figure 3). The cleavage of the P–N linkage was slowed down as the $[H^+]$ decreased, and the plots of the k_{obs} against $[H^+]$ exhibited a good inverse relationship within pH 4.0–4.9 for both **TFO8** and **TFO4**.

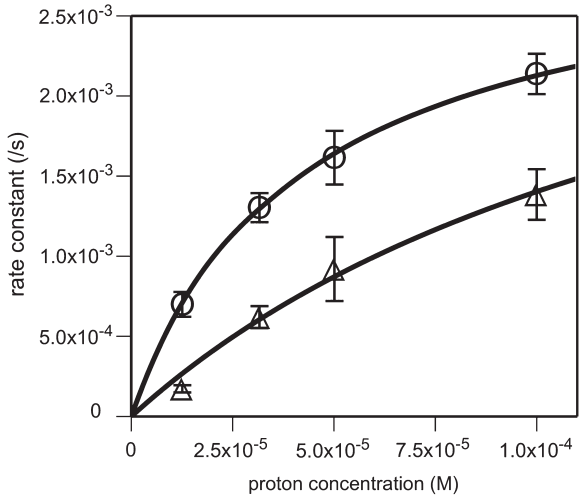

Figure 3. Pseudo-first order rate constants (k_{obs}) of **TFO8** (open circles) and **TFO4** (open triangles) in the triplex form plotted against proton concentration ([H^+]) at 40°C. Error bars indicate standard deviation ($n = 3$). Conditions: 140 mM KCl, 10 mM $MgCl_2$, 1.0 mM sodium phosphate buffer, 10 mM sodium citrate-based buffer, 3.35 μM each strand, the final pH 4.0, 4.3, 4.5 and 4.9.

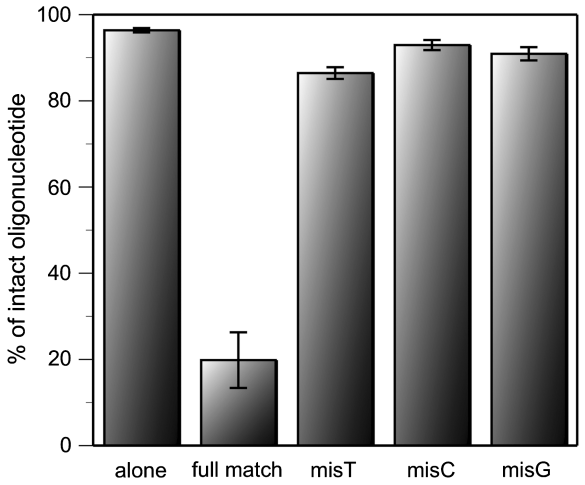

Figure 4. Percent of intact **TFO8** in the presence of the full match or mismatch target dsDNA, misT, misC, and misG, or the absence of the target dsDNA (alone). Error bars indicate standard deviation ($n = 3$–4). Conditions: 140 mM KCl, 10 mM $MgCl_2$, 1.0 mM sodium phosphate buffer, 10 mM sodium citrate–HCl buffer, 3.35 μM each strand, the final pH 3.3, 40°C, reaction time 2 min.

Sequence selectivity

As we found out that **TFO8** had a great potential as a DNA-detecting probe, its sequence selectivity was evaluated. **TFO8** was treated with the full match target dsDNA or target dsDNAs containing different base pairs in the middle of the sequence (misT, misC and misG, Figure 1) at pH 3.3 to compare with **TFO***, whose sequence selectivity was evaluated at the previously reported conditions (28). While **TFO*** exhibited high sequence selectivity after 10 min of incubation under the conditions (28), **TFO8** showed even higher contrast within only 2 min (Figure 4). To gather information on the origin of the sequence selectivity, the thermal stability of the mismatch triplexes containing **TFO8** was evaluated by means of the UV melting experiments (Supplementary Figure S1E). The triplex stability of the mismatch triplexes was revealed to be quite low compared to that of the full match triplex (T_m: full match, 61°C; misT, 23°C; misC, 35°C; misG, 27°C, Supplementary Figure S1E).

DISCUSSION

Effects of 5′-elongation flanking the P–N linkage

In the presence of the target dsDNA, **TFO1** containing 5′-aminomethyl-2′,4′-BNA (X^2) exhibited comparable reactivity to **TFO***, while unbridged **TFO2** containing 5′-aminomethyl-DNA (X^3) exhibited higher reactivity than **TFO***. This relationship was different from the relationship between 5′-amino-2′,4′-BNA (NH)-modified TFO and 5′-amino-DNA (NH)-modified TFO, where 2′,4′-BNA modification brought somewhat higher reactivity (28). We suppose that the combination of restriction of the sugar conformation to the N-type and the insertion of a methylene group was incompatible for the cleaving reaction triggered by triplex formation.

In the absence of the target dsDNA, **TFO1** and **TFO2** both exhibited higher reactivity than any other TFOs. This result is explainable considering the less steric crowding around their P-N linkages. Thus, the protonation on the phosphoramidate and subsequent nucleophilic attack of water might be easier, leading to higher reactivity in their single-stranded states.

Effects of introduction of 2′,4′-BNA/LNA to neighboring residues

Although the sugar conformation in the third strand of a triplex is still ambiguous, there are reports pointing out that the sugar conformation is altered depending on the positions and/or patterns of 2′,4′-BNA/LNA modifications (42,43). Similarly, 2′,4′-BNA/LNA modifications would affect differently on the strain of the neighboring P-N linkage depending on their modification positions. As a result, the 2′,4′-BNA/LNA (Y) modification at the 3′-neighboring residue of 5′-amino-2′,4′-BNA (X^1) (**TFO4**) is assumed to have increased the strain on the P–N linkage appropriately while the modification at the 5′-neighboring residue (**TFO3** and **TFO5**) almost completely relaxed the strain. As the separation of the 2′,4′-BNA/LNA from the 5′-amino-2′,4′-BNA residue (**TFO6**) led to high reactivity in the presence of the target dsDNA, the introduction of 2′,4′-BNA/LNA at the 5′-neighbor of the 5′-amino-2′,4′-BNA seems to be critically unfavorable for the cleavage of the P–N linkage.

Effects of introduction of 2′,5′-linked DNA to neighboring residues

Since 2′,5′-linked DNA has a different phosphodiester topology, the introduction of 2′,5′-linked DNA in the neighborhood of the P–N linkage may affect the microenvironment around the linkage. In fact, significantly higher reactivity than **TFO*** was observed for **TFO8** in

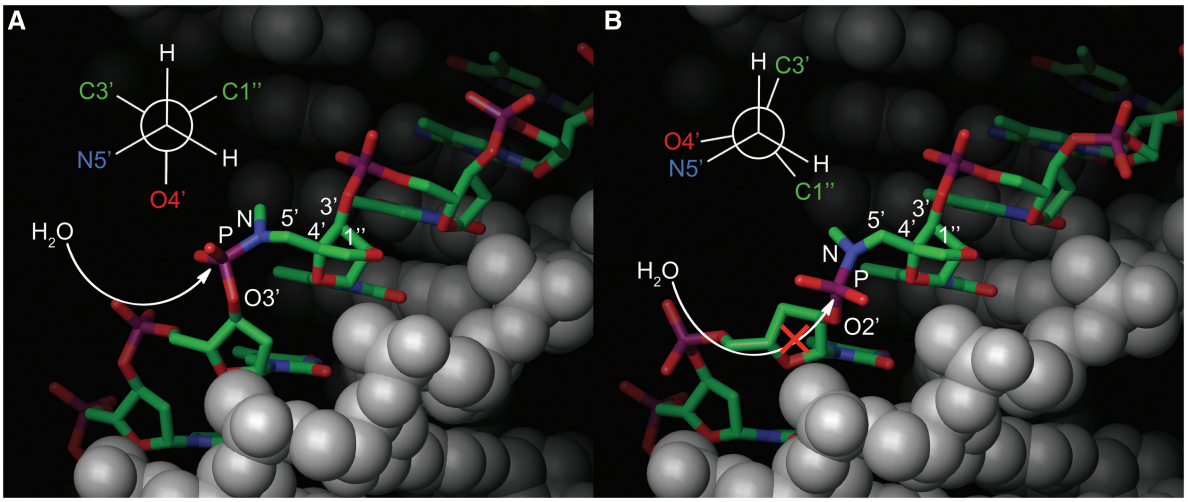

Figure 5. Triplex structure of **TFO*** (**A**) and **TFO7** (**B**). The third strands are rendered as stick models colored by elements, and their target dsDNAs are rendered as gray colored CPK model. In **TFO***, the γ dihedral angle (N5′-C5′-C4′-C3′) was estimated to adopt a *+sc* orientation while that of **TFO7** was estimated to adopt a *+ac* (see Newman's projection formula, *+sc*; 30–90°, *+ac*; 90°–150°). The access of water molecules seems easy for **TFO***, although their attack from the backside of the P-N linkage seems sterically forbidden for **TFO7**.

the presence of the target dsDNA, while the cleavage of the P–N linkage brought by the target dsDNA was completely extinguished in the case of **TFO7** and **TFO9**.

Molecular modeling of the triplex structures containing each TFO (**TFO***, **TFO7**, **TFO8** and **TFO9**) brought us important suggestions to understand the results. First, the phosphorus atom of the P–N linkage in **TFO7** and **TFO9** was linked to the O2′, drawing the P–N linkage into the inner side of the triplex, and the backside of the P–N linkage was well shielded, which would make it difficult for water molecules to access the phosphorus atom (Figure 5). On the other hand, the P–N linkages of **TFO*** and **TFO8** (Figure 5 and Supplementary Figure S4A) were located outside the triplex, and the access of water molecules seemed easier. Second, the modeling also suggested that the γ dihedral angle (N5′-C5′-C4′-C3′) of the 5′-amino-2′,4′-BNA residue in **TFO7**, and **TFO9** adopted a *+ac* orientation (Figure 5 and Supplementary Figure S4B), while that for **TFO*** and **TFO8** was estimated to adopt a *+sc* orientation. According to the report made by Letsinger *et al.*, ^{1}H-NMR study on the solution structure of the single-stranded thymidil 5′-amino-DNA dimer (5′-TX-3′) revealed that the *+sc* population is low (44). As the single-stranded structure is assumed to reflect the less strained structure, the *+sc* orientation may be thermodynamically less favorable. Considering the results of the modeling studies that the γ dihedral angle of the highly reactive TFOs was estimated to adopt a *+sc* orientation in triplex state, the dihedral angle seems to be strongly related to the strain on the P–N linkage by affecting, for example, the π conjugation between the P–N linkage.

Effect of pH on the reactivity

Hydrolysis experiments were performed at different pH to gather more information on the accelerated cleavage of **TFO8**. Although linearity might have observed in k_{obs} versus [H$^+$] as other group reported on the hydrolysis of N3′→P5′ phosphoramidate dinucleotide (45), inverse relationships were observed when the triplex was formed under our conditions (Figure 3). At pH 4.0–4.9, there is assumed to be the equilibrium between the electrically neutral phosphoramidate (TFO_{neu}) and electrically negative one (TFO_{ani}), and the reactant of the P–N cleavage reaction would be only the TFO_{neu} as shown in Scheme 4 (45). Accordingly, the reaction rate (v) would be expressed as Equations 1 and 2, where c, [TFO_{neu}], and k_1' represent the concentration of total TFO, that of TFO with the neutral phosphoramidate (Scheme 4) and first

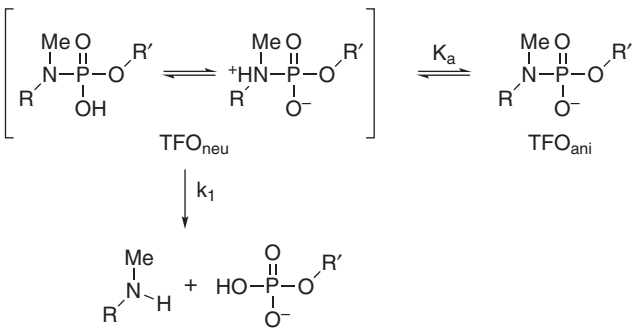

Scheme 4. Equilibrium of phosphoramidates related to the cleavage of the P–N linkage under mild acidic conditions.

$$v = k_1[TFO_{neu}][H_2O] \quad (1)$$

$$v \cong k_1'[TFO_{neu}] \quad (2)$$

$$[\mathrm{TFO}_{neu}] = c \times \frac{[\mathrm{H}^+]}{[\mathrm{H}^+] + K_a} \quad (3)$$

$$v \cong k_{obs} \times c \quad (4)$$

$$k_{obs} = k_1' \times \frac{[\mathrm{H}^+]}{[\mathrm{H}^+] + K_a} \quad (5)$$

$$k_{obsTFO8} = \frac{3.0 \times 10^{-3} \times [\mathrm{H}^+]}{[\mathrm{H}^+] + 4.3 \times 10^{-5}} \quad (6)$$

$$k_{obsTFO4} = \frac{3.6 \times 10^{-3} \times [\mathrm{H}^+]}{[\mathrm{H}^+] + 1.6 \times 10^{-4}} \quad (7)$$

order rate constant in triplex form at 40°C, respectively. From the T_m analysis, the total concentration of **TFO8** and **TFO4** was assumed to be approximately equal to the concentration of each TFO in triplex form at pH 4.0–4.9. When K_a is defined as the acid dissociation constant of the corresponding TFO_{neu} in triplex form at 40°C (Scheme 4), the inverse proportion of k_{obs} to $[H^+]$ led to an estimation of the pK_a, which were calculated from the curve fitting [Figure 3 and Equations 3–5]. The obtained equations containing the parameters for **TFO8** and **TFO4** are provided in Equations 6 and 7, respectively. The estimated pK_as were 4.4 (for **TFO8**) and 3.8 (for **TFO4**), and these values were significantly higher than those of simple phosphoramidate *N,O*-diesters (p$K_a \cong$ 2–3) (45–47). The accelerated hydrolysis may be explained by the higher estimated pK_a, which increases the proportion of TFO_{neu} to TFO_{ani}. The phosphorus atom and nitrogen atom in the P–N linkage are able to form an additional π bond (46), and the highly reactive TFOs would have a strained P–N linkage whose conjugation is restricted, resulting in higher basicity of the phosphoramidate. The consideration made by the modeling studies, which indicated the importance of the γ dihedral angle on the reactivity, seems to be reasonable because the dihedral angle would have a significant impact on the P–N conjugation.

Potential of TFO8 as analytical tool

To elucidate the detail properties of **TFO8** as an analytical tool, its sequence selectivity was evaluated. Comparison

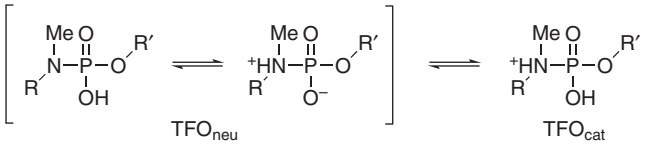

Scheme 5. Equilibrium between the neutral form and the cationic form of phosphoramidates.

with a previous report (28) obviously declared that **TFO8** had much higher potential as an analytical tool because **TFO8** was cleaved to the same level with **TFO*** within 5 times shorter reaction time, even with lower background noise (in the presence of the mismatch target or the absence of the target dsDNA, Figure 4). The UV melting experiments supported the results of the hydrolysis experiments by indicating that the mismatch triplexes were significantly unstable (Supplementary Figure S1E). Although the kinetic study was not performed at pH 3.3 conditions, the half-life of **TFO8** in the presence of the full match target dsDNA could be estimated from Figure 4. As the intact **TFO8** was ~20% after 2 min of incubation, the half-life was estimated to be <1 min. The estimated half-life was obviously shorter than that expected from Equation 6 (~4 min). This result may be explained by the emerging of the cationic phosphoramidate as a rather reactive substrate than the neutral phosphoramidate under the conditions (Scheme 5). This form of phosphoramidate was not included in the prerequisite of the Equation 6, and this may be the reason why the reactivity at pH 3.3 was assumed to be much higher than expected.

General overview

We successfully demonstrated that the acid-mediated cleavage of the P–N linkage triggered by triplex formation reflects the microenvironment around the P–N linkage. From the present study, we found that the introduction of 2′,5′-linked DNA to the 3′-neighboring residue of 5′-amino-2′,4′-BNA gave the highest reactivity with high sequence selectivity, and we can conclude that a probe with the modification is promising as a dsDNA-detecting tool.

Through this investigation, we succeeded in supporting our concept on the hydrolysis acceleration triggered by triplex formation. The pK_a of phosphoramidates seemed to have a positive correlation with the cleavage rate, which would be reflecting the change in the microenvironment around the P–N linkage. This observation indicates the direction of rational design of further chemical modifications bringing higher reactivity with lower background noise.

We and other groups have made efforts to expand the target sequences in triplex-based technologies through the designs and syntheses of TFOs containing unnatural nucleobases that recognize pyrimidine interruption in a homopurine strand (48–54). Therefore, this triplex-based DNA analysis tool would also be applicable to the analysis of pyrimidine-containing strand in near future. We are now optimizing this analytical tool for key

biomedical applications, such as detecting single nucleotide polymorphisms.

SUPPLEMENTARY DATA

Supplementary Data are available at NAR Online.

FUNDING

Precursory Research for Embryonic Science and Technology (PRESTO to S.O.); Japan Science and Technology Agency, Creation and Support Program for Start-ups from Universities (to T.I. and S.O.); Japan Society for the Promotion of Science, KAKENHI; Ministry of Education, Culture Sports, Science and Technology, Japan. Funding for open access charge: Japan Society of Promotion of Science.

Conflict of interest statement. None declared.

REFERENCES

1. Brunner,J., Mokhir,A. and Kraemer,R. (2003) DNA-templated metal catalysis. *J. Am. Chem. Soc.*, **125**, 12410–12411.
2. Abe,H. and Kool,E.T. (2004) Destabilizing universal linkers for signal amplification in self-ligating probes for RNA. *J. Am. Chem. Soc.*, **126**, 13980–13986.
3. Boll,I., Krämer,R., Brunner,J. and Mokhir,A. (2005) Templated metal catalysis for single nucleotide specific DNA sequence detection. *J. Am. Chem. Soc.*, **127**, 7849–7856.
4. Ficht,S., Dose,C. and Seitz,O. (2005) As fast and selective as enzymatic ligations: unpaired nucleobases increase the selectivity of DNA-controlled native chemical PNA ligation. *ChemBioChem.*, **6**, 2098–2103.
5. Dose,C., Ficht,S. and Seitz,O. (2006) Reducing product inhibition in DNA-template-controlled ligation reactions. *Angew. Chem. Int. Ed.*, **45**, 5369–5373.
6. Franzini,R.M. and Kool,E.T. (2008) Organometallic activation of a fluorogen for templated nucleic acid detection. *Org. Lett.*, **10**, 2935–2938.
7. Xu,Y., Karalkar,N.B. and Kool,E.T. (2001) Nonenzymatic autoligation in direct three-color detection of RNA and DNA point mutations. *Nat. Biotechnol.*, **19**, 148–152.
8. Sando,S. and Kool,E.T. (2002) Quencher as leaving group: Efficient detection of DNA-joining reactions. *J. Am. Chem. Soc.*, **124**, 2096–2097.
9. Cai,J., Li,X., Yue,X. and Taylor,J.S. (2004) Nucleic acid-triggered fluorescent probe activation by the Staudinger reaction. *J. Am. Chem. Soc.*, **126**, 16324–16325.
10. Cai,J., Li,X. and Taylor,J.S. (2005) Improved nucleic acid triggered probe activation through the use of a 5-thiomethyluracil peptide nucleic acid building block. *Org. Lett.*, **7**, 751–754.
11. Grossmann,T.N. and Seitz,O. (2006) DNA-catalyzed transfer of a reporter group. *J. Am. Chem. Soc.*, **128**, 15596–15597.
12. Abe,H. and Kool,E.T. (2006) Flow cytometric detection of specific RNAs in native human cells with quenched autoligating FRET probes. *Proc. Natl Acad. Sci. USA*, **103**, 263–268.
13. Ogasawara,S. and Fujimoto,K. (2006) SNP genotyping by using photochemical ligation. *Angew. Chem. Int. Ed.*, **45**, 4512–4515.
14. Yoshimura,Y., Noguchi,Y., Sato,H. and Fujimoto,K. (2006) Template-directed DNA photoligation in rapid and selective detection of RNA point mutations. *ChemBioChem.*, **7**, 598–601.
15. Pianowski,Z.L. and Winssinger,N. (2007) Fluorescence-based detection of single nucleotide permutation in DNA *via* catalytically templated reaction. *Chem. Commun.*, 3820–3822.
16. Franzini,R.M. and Kool,E.T. (2008) 7-Azidomethoxy-coumarins as profluorophores for templated nucleic acid detection. *ChemBioChem.*, **9**, 2981–2988.
17. Peng,X. and Greenberg,M.M. (2008) Facile SNP detection using bifunctional, cross-linking oligonucleotide probes. *Nucleic Acids Res.*, **36**, e31.
18. Abe,H., Kondo,Y., Jinmei,H., Abe,N., Furukawa,K., Uchiyama,A., Tsuneda,S., Aikawa,K., Matsumoto,I. and Ito,Y. (2008) Rapid DNA chemical ligation for amplification of RNA and DNA signal. *Bioconjugate Chem.*, **19**, 327–333.
19. Furukawa,K., Abe,H., Wang,J., Uda,M., Koshino,H., Tsuneda,S. and Ito,Y. (2008) Reduction-triggered red fluorescent probes for dual-color detection of oligonucleotide sequences. *Org. Biomol. Chem.*, **7**, 671–677.
20. Dose,C. and Seitz,O. (2008) Single nucleotide specific detection of DNA by native chemical ligation of fluorescence labeled PNA-probes. *Bioorg. Med. Chem.*, **16**, 65–77.
21. Grossmann,T.N., Röglin,L. and Seitz,O. (2008) Target-catalyzed transfer reactions for the amplified detection of RNA. *Angew. Chem. Int. Ed.*, **47**, 7119–7122.
22. Grossmann,T.N. and Seitz,O. (2009) Nucleic acid templated reactions: consequences of probe reactivity and readout strategy for amplified signaling and sequence selectivity. *Chem. Eur. J.*, **15**, 6723–6730.
23. Franzini,R.M. and Kool,E.T. (2009) Efficient nucleic acid detection by templated reductive quencher release. *J. Am. Chem. Soc.*, **131**, 16021–16023.
24. Gartner,Z.J. and Liu,D.R. (2001) The generality of DNA-templated synthesis as a basis for evolving non-natural small molecules. *J. Am. Chem. Soc.*, **123**, 6961–6963.
25. Gartner,Z.J., Kanan,M.W. and Liu,D.R. (2002) Multistep small-molecule synthesis programmed by DNA templates. *J. Am. Chem. Soc.*, **124**, 10304–10306.
26. Gartner,Z.J., Tse,B.N., Grubina,R., Doyon,J.B., Snyder,T.M. and Liu,D.R. (2004) DNA-templated organic synthesis and selection of a library of macrocycles. *Science*, **305**, 1601–1605.
27. Heitner,T.R. and Hansen,N.J.V. (2009) Streamlining hit discovery and optimization with a yoctoliter scale DNA reactor. *Expert Opin. Drug Discov.*, **4**, 1201–1213.
28. Obika,S., Tomizu,M., Negoro,Y., Orita,A., Nakagawa,O. and Imanishi,T. (2007) Double-stranded DNA-templated oligonucleotide digestion triggered by triplex formation. *ChemBioChem.*, **8**, 1924–1928.
29. Bannwarth,W. (1988) Solid-phase synthesis of oligodeoxynucleotides containing phosphoramidate internucleotide linkages and their specific chemical cleavage. *Helv. Chim. Acta*, **71**, 1517–1527.
30. Obika,S., Tomizu,M., Negoro,Y., Osaki,T., Orita,A., Ueyama,Y., Nakagawa,T. and Imanishi,T. (2007) Acid-mediated cleavage of oligonucleotide P3'→N5' phosphoramidates triggered by sequence-specific triplex formation. *Nucleosides, Nucleotides, Nucleic Acids*, **26**, 893–896.
31. Obika,S., Nanbu,D., Hari,Y., Morio,K., In,Y., Ishida,T. and Imanishi,T. (1997) Synthesis of 2′-*O*,4′-*C*-methyleneuridine and -cytidine. Novel bicyclic nucleosides having a fixed C3′-endo sugar puckering. *Tetrahedron Lett.*, **38**, 8735–8738.
32. Obika,S., Nanbu,D., Hari,Y., Andoh,J., Morio,K., Doi,T. and Imanishi,T. (1998) Stability and structural features of the duplexes containing nucleoside analogues with a fixed N-type conformation, 2′-*O*,4′-*C*-methyleneribonucleosides. *Tetrahedron Lett.*, **39**, 5401–5404.
33. Singh,S.K., Nielsen,P., Koshkin,A.A. and Wengel,J. (1998) LNA (locked nucleic acids): Synthesis and high-affinity nucleic acid recognition. *Chem. Commun.*, 455–456.
34. Obika,S., Uneda,T., Sugimoto,T., Nanbu,D., Minami,T., Doi,T. and Imanishi,T. (2001) 2′-*O*,4′-*C*-methylene bridged nucleic acid (2′,4′-BNA): Synthesis and triplex-forming properties. *Bioorg. Med. Chem.*, **9**, 1001–1011.
35. Lalitha,V. and Yathindra,N. (1995) Even nucleic acids with 2′,5′-linkages facilitates duplexes and structural polymorphism: Prospects of 2′,5′-oligonucleotides as antigene/antisense tool in gene regulation. *Curr. Sci.*, **68**, 68–75.
36. Obika,S., Hiroto,A., Nakagawa,O. and Imanishi,T. (2005) Promotion of stable triplex formation by partial incorporation of 2′,5′-phosphodiester linkages into triplex-forming oligonucleotides. *Chem. Commun.*, 2793–2795.

37. Koshkin,A.A., Fensholdt,J., Pfundheller,H.M. and Lomholt,C. (2001) A simplified and efficient route to 2′-*O*, 4′-*C*-methylene-linked bicyclic ribonucleosides (locked nucleic acid). *J. Org. Chem.*, **66**, 8504–8512.
38. Kofoed,T., Rasmussen,P.B., Valentin-Hansen,P. and Pedersen,E.B. (1997) Oligodeoxynucleotides with extended 3′- and 5′-homologous internucleotide linkages. *Acta Chem. Scand.*, **51**, 318–324.
39. Plum,G.E., Park,Y., Singleton,S.F., Dervan,P.B. and Bresulauer,K.J. (1990) Thermodynamic characterization of the stability and the melting behavior of a DNA triplex: A spectroscopic and calorimetric study. *Proc. Natl Acad. Sci. USA*, **87**, 9436–9440.
40. Roberts,R.W. and Crothers,D.M. (1996) Prediction of the stability of DNA triplexes. *Proc. Natl Acad. Sci. USA*, **93**, 4320–4325.
41. Singleton,S.F. and Dervan,P.B. (1992) Influence of pH on the equilibrium association constants for oligodeoxyribonucleotide-directed triple helix formation at single DNA sites. *Biochemistry*, **31**, 10995–11003.
42. Sun,B., Babu,B.R., Sørensen,M.D., Zakrzewska,K., Wengel,J. and Sun,J. (2004) Sequence and pH effects of LNA-containing triple helix-forming oligonucleotides: Physical chemistry, biochemistry, and modeling studies. *Biochemistry*, **43**, 4160–4169.
43. Sørensen,J.J., Nielsen,J.T. and Petersen,M. (2004) Solution structure of a dsDNA:LNA triplex. *Nucleic Acids Res.*, **32**, 6078–6085.
44. Nottoli,E.M., Lambert,J.B. and Letsinger,R.L. (1977) Study of conformational changes induced on substituting NH for O at C(5') of thymidine nucleosides and nucleotides. *J. Am. Chem. Soc.*, **99**, 3486–3491.
45. Ora,M., Mattila,K., Lönnberg,T., Oivanen,M. and Lönnberg,H. (2002) Hydrolytic reactions of diribonucleoside 3′,5′-(3′-*N*-phosphoramidates): Kinetics and mechanism for the P–O and P–N bond cleavage of 3′-amino-3′-deoxyuridylyl-3′,5′-uridine. *J. Am. Chem. Soc.*, **124**, 14364–14372.
46. Preobrazhenskaya,N.N. (1972) Reactions of phosphoramidic acids. *Russ. Chem. Rev.*, **41**, 54–65.
47. Sampson,E.J., Fedor,J., Benkovic,P.A. and Benkovic,S.J. (1973) Intramolecular and divalent metal ion catalysis. The hydrolytic mechanism of *O*-phenyl *N*-(glycyl)phosphoramidate. *J. Org. Chem.*, **38**, 1301–1306.
48. Prévot-Halter,I. and Leumann,C.J. (1999) Selective Recognition of a C-G base-pair in the parallel DNA triple-helical binding motif. *Bioorg. Med. Chem. Lett.*, **9**, 2657–2660.
49. Guianvarc'h,D., Benhida,R., Fourrey,J., Maurisse,R. and Sun,J. (2001) Incorporation of a novel nucleobase allows stable oligonucleotide-directed triple helix formation at the target sequence containing a purine·pyrimidine interruption. *Chem. Commun.*, 1814–1815.
50. Obika,S., Hari,Y., Sekiguchi,M. and Imanishi,T. (2001) A 2,4-bridged nucleic acid containing 2-pyridone as a nucleobase: efficient recognition of a CG interruption by triplex formation with a pyrimidine motif. *Angew. Chem. Int. Ed.*, **40**, 2079–2081.
51. Guianvarc'h,D., Fourrey,J., Maurisse,R., Sun,J. and Benhida,R. (2002) Synthesis, incorporation into triplex-forming oligonucleotide, and binding properties of a novel 2′-deoxy-*C*-nucleoside featuring a 6-(thiazolyl-5)benzimidazole nucleobase. *Org. Lett.*, **4**, 4209–4212.
52. Obika,S., Hari,Y., Sekiguchi,M. and Imanishi,T. (2002) Stable oligonucleotide-directed triplex formation at target sites with CG interruptions: Strong sequence-specific recognition by 2′,4′-bridged nucleic-acid-containing 2-pyridones under physiological conditions. *Chem. Eur. J.*, **8**, 4796–4802.
53. Rusling,D.A., Powers,V.E.C., Ranasinghe,R.T., Wang,Y., Osborne,S.D., Brown,T. and Fox,K.R. (2005) Four base recognition by triplex-forming oligonucleotides at physiological pH. *Nucleic Acids Res.*, **33**, 3025–3032.
54. Wang,Y., Rusling,D.A., Powers,V.E.C., Lack,O., Osborne,S.D., Fox,K.R. and Brown,T. (2005) Stable recognition of TA interruptions by triplex forming oligonucleotides containing a novel nucleoside. *Biochemistry*, **44**, 5884–5892.